**Published paper**
Shao, Ling, Wang, Jingnan, Kirenko, Ihor and de Haan, Gerard (2011) *Quality Adaptive Least Squares Trained Filters for Video Compression Artifacts Removal Using a No-reference Block Visibility Metric.* Journal of Visual Communication and Image Representation, 22 (1). pp. 23-32.
http://dx.doi.org/10.1016/j.jvcir.2010.09.007

# Quality Adaptive Least Squares Trained Filters for Video Compression Artifacts Removal Using a No-reference Block Visibility Metric

Ling Shao*, Jingnan Wang†, Ihor Kirenko‡, Gerard de Haan‡

* Department of Electronic & Electrical Engineering, The University of Sheffield, UK

† EECS Department, Northwestern University, USA

‡ Philips Research Laboratories, Eindhoven, The Netherlands

## Abstract

Compression artifacts removal is a challenging problem because videos can be compressed at different qualities. In this paper, a least squares approach that is self-adaptive to the visual quality of the input sequence is proposed. For compression artifacts, the visual quality of an image is measured by a no-reference block visibility metric. According to the blockiness visibility of an input image, an appropriate set of filter coefficients that are trained beforehand is selected for optimally removing coding artifacts and reconstructing object details. The performance of the proposed algorithm is evaluated on a variety of sequences compressed at different qualities in comparison to several other deblocking techniques. The proposed method outperforms the others significantly both objectively and subjectively.

## 1. Introduction

Due to the bandwidth limit of the broadcasting channels and the capacity limit of the storage media, video materials are always compressed with various compression standards, such as MPEG-2 and MPEG-4. These block transform based codecs divide the image or video frame into non-overlapping blocks (usually with the size of 8 x 8 pixels), and apply discrete cosine transform (DCT) on them. The DCT coefficients of neighboring blocks are thus quantized independently. At high or medium compression rates, the coarse quantization will result in various noticeable coding artifacts, such as blocking, ringing and mosquito artifacts. Coding artifact reduction techniques are used to remove various artifacts. Among the coding artifacts, blockiness which appears as discontinuities along block boundaries is the most annoying. Therefore, an in-loop deblocking filter is specified for H.264/AVC to reduce blocking artifacts using coding parameters inside the encoder. However, JPEG compressed images and MPEG-2 compressed videos will remain ubiquitous, which makes post-processing aimed at the elimination of coding artifacts still a critical and indispensable solution.

Most coding artifact reduction techniques based on post-processing, e.g. [1-6], are designed according to heuristic tuning and testing, which takes a lot of time and is not always effective. Recently, classification-based least squares trained filters (TF), initially designed for image resolution upscaling [7], have been proposed for optimally removing digital coding artifacts [8, 9]. The momentary filter coefficients, during artifact reduction, depend on the local content of the image, which can be classified into classes based on the image characteristics in the filter aperture. To obtain the optimized filter coefficients, a training process should be performed in advance. The training process employs the combination of original images and the degraded versions of those original images as the training material and uses the Least Squares (LS) criterion to get the optimal coefficients, which is computationally intensive due to the large number of classes. Fortunately, the training process only needs to be performed off-line and once. The method introduced in [8] produces promising results, when the quality of the test sequence is similar to that of the source sequences used during training. It is because a fixed level of compression is adopted for degrading the original images. In this paper, we propose to train the algorithm on a range of compression levels and to select the most suitable set of filter coefficients for the test sequence. To do that, a quality (or blockiness) metric is required to indicate the quality level of the test sequence.

The main contribution of the paper is the use of the no-reference blockiness visibility metric for the least squares trained filters which makes the algorithm capable of dealing with various qualities of input sequences.

In the following, we first briefly introduce the classification based least squares filters in Section 2. Section 3 analyzes the properties of the algorithm on coding artifact reduction, when the original images are degraded with different qualities and using different compression methods. The new trained filters that are adaptive to the visual quality of the input sequence, which is indicated by a block visibility metric, are proposed in Section 4. We evaluate the performance of the proposed algorithm in contrast to the original trained filters and other adaptive filters. Finally, we draw our conclusion in Section 5.

## 2. Trained Filters

### 2.1 Introduction of Trained Filters

The Least Squares algorithm is composed of two parts: the training process and the filtering process. To obtain the momentary filter coefficients, a training process should be performed in advance. Figure 1 shows the training process of the trained filters. Original images are first degraded according to the specification of the application. The training process employs the original video sequences and corresponding degraded video sequences as the training material and uses the Least Squares criterion to get the optimal coefficients, which is computational intensive due to the large number of classes. Fortunately, it needs to be performed only once. There are various ways to degrade the original high quality sequences. Generally speaking, the degradation during the training process is the inverse of the enhancement that one expects during the filtering process. In this paper, two kinds of degradation methods are applied, that is JPEG compression and MPEG compression. We refer to the images after degradation as degraded images. In the degraded images, each pixel and the pixels in its vicinity are characterized using a specific classification method. All the pixels and their neighborhoods belonging to a specific class and their corresponding pixels in the original images are accumulated, and the optimal coefficients are obtained by making the Mean Square Error (MSE) minimized statistically.

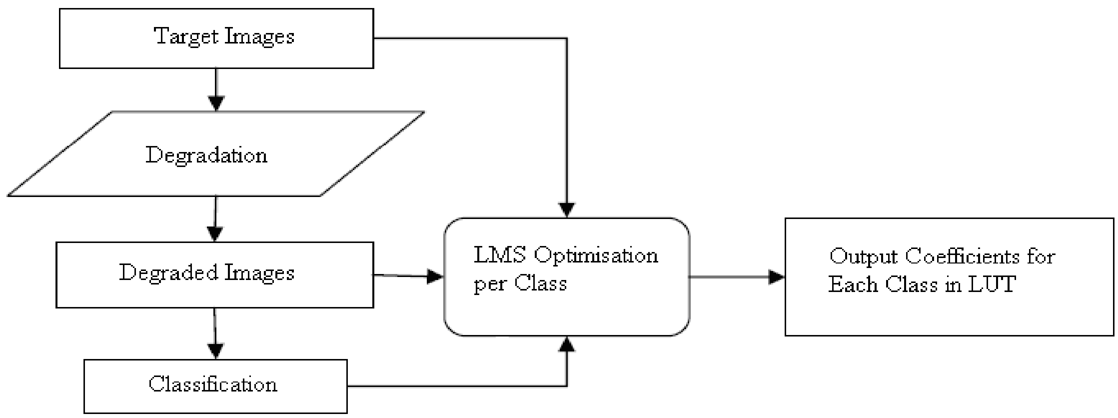


**Figure 1: Training process of the trained filters.**

Let $F_{D,c}$, $F_{R,c}$ be the apertures of the degraded images and the reference images for a particular class $c$, respectively. Then the filtered pixel $F_{F,c}$ can be obtained by the desired optimal coefficients as follows:

$$F_{F,c} = \sum_{i=1}^{n} w_c(i) F_{D,c}(i, j) \tag{1}$$

where $w_c(i), i \in [1...n]$ are the desired coefficients, $n$ is the number of pixels in the aperture, and $j$ indicates a particular aperture belonging to class $c$. The summed square error between the filtered pixels and the reference pixels is:

$$e^2 = \sum_{j=1}^{Nc} (F_{R,c} - F_{F,c})^2 = \sum_{j=1}^{Nc} \left[ F_{R,c}(j) - \sum_{i=1}^{n} w_c(i) F_{D,c}(i, j) \right]^2 \tag{2}$$

where $N_c$ represents the number of training samples belonging to class $c$. To minimize $e^2$, the first derivative of $e^2$ to $w_c(k), k \in [1...n]$ should be equal to zero.

$$\frac{\partial e^2}{\partial w_c(k)} = \sum_{j=1}^{Nc} 2F_{D,c}(k,j)\left[F_{R,c}(j) - \sum_{i=1}^{n} w_c(i)F_{D,c}(i,j)\right] = 0 \quad (3)$$

By solving the above equation using Gaussian elimination, we will get the optimal coefficients as follows:

$$\begin{bmatrix} w_c(1) \\ w_c(2) \\ \cdots \\ w_c(n) \end{bmatrix} = \begin{bmatrix} \sum_{j=1}^{N_c} F_{D,c}(1,j)F_{D,c}(1,j) & \cdots & \sum_{j=1}^{N_c} F_{D,c}(1,j)F_{D,c}(n,j) \\ \sum_{j=1}^{N_c} F_{D,c}(2,j)F_{D,c}(1,j) & \cdots & \sum_{j=1}^{N_c} F_{D,c}(2,j)F_{D,c}(n,j) \\ \cdots & \cdots & \cdots \\ \sum_{j=1}^{N_c} F_{D,c}(n,j)F_{D,c}(1,j) & \cdots & \sum_{j=1}^{N_c} F_{D,c}(n,j)F_{D,c}(n,j) \end{bmatrix}^{-1} \begin{bmatrix} \sum_{j=1}^{N_c} F_{D,c}(1,j)F_{R,c}(j) \\ \sum_{j=1}^{N_c} F_{D,c}(2,j)F_{R,c}(j) \\ \cdots \\ \sum_{j=1}^{N_c} F_{D,c}(n,j)F_{R,c}(j) \end{bmatrix} \quad (4)$$

The LS optimized coefficients for each class are then stored in a look-up table (LUT) for future use.

Figure 2 shows the filtering process of the algorithm using the optimized coefficients. For each pixel to be filtered, the neighboring pixels are classified in the same manner as during training. The coefficients are retrieved from the LUT based on the classification. The pixels are then filtered using the optimized coefficients.

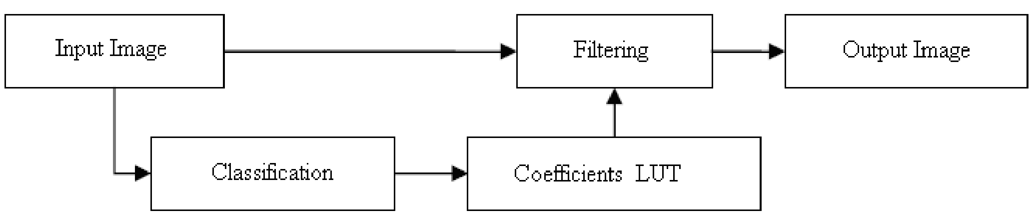


**Figure 2: Filtering process of the trained filters.**

### 2.2 Pixel Classification Methods

#### 2.2.1 Adaptive Dynamic Range Coding Based Classification

As stated in the previous section, the momentary filter coefficients, during filtering, depend on the local characteristics of the image, which can be classified based on the pattern of the image region and structure information is always important for either low-pass filtering or high-pass filtering. Adaptive Dynamic Range Coding (ADRC) [10] is proposed as a powerful method for representing the structure of a region because of its high efficiency and simplicity. The ADRC code of each pixel $x_i$ in an observation aperture is defined as: ADRC ($x_i$) =0, if V ($x_i$) $\leqslant$ $V_{av}$ ; 1, otherwise, where V($x_i$) is the value of pixel $x_i$ , and $V_{av}$ is the average of all the pixel values in the aperture. Figure 3 shows a diagram of the ADRC code on a 3x3 block.

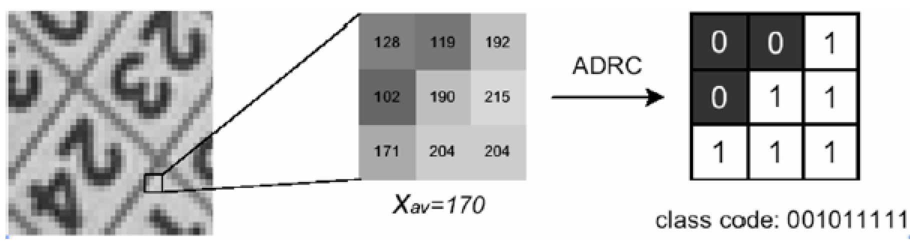


**Figure 3: The ADRC code of a 3x3 block.**

#### 2.2.2 Improved ADRC Based Classification Methods

Obviously, only using structure for classification is not sufficient, because the structure of coding artifacts could be exactly the same as that of object details. To obtain better performance, several additional criteria have been proposed [8]. For example, considering that high contrast structures and low contrast structures should be treated differently, dynamic range (DR) can be added to ADRC. DR is simply the absolute difference between the maximum and minimum pixel values of the image region.  Several other ancillary classification methods are in use, such as local entropy [1], which is an activity measure for distinguishing complex regions from uniform regions. The entropy value is calculated on the probability density functions of the pixel intensity distribution. The local entropy of a region can be defined as follows:

$$H = -\sum_{i=1}^{N} P_R(i) \log_2 P_R(i) \tag{5}$$

Where $i$ indicates the bin index, $P_R(i)$ is the probability of pixels having a value in the range of bin $i$ and R is a local region inside which the entropy is calculated.

Another measure is called Mean Absolute Gradient (MAG) for determining the complexity of a region. MAG is defined as follows:

$$MAG = \frac{1}{N-1}\sum_{i=1}^{N-1}\left|F(0) - F(i)\right| \tag{6}$$

where $F(i)$ denotes the intensity value of a pixel in a region, $F(0)$ is the intensity of the pixel in the center, and $N$ is the number of pixels in the region. Standard Deviation (STD) is employed as another complexity metric for a local region.

Structure information using ADRC coupled with one of the complexity measures described above will be used for classification. For all the above complexity measures, a 13 pixel diamond-shaped aperture, as depicted in Figure 4, is used for both classification and filtering. Therefore, 12 bits are needed for the ADRC code, because 1 bit can be saved using bit-inversion. And, 2 more bits are used for representing the complexity of a region. So, in total 14 bits are used for classification.

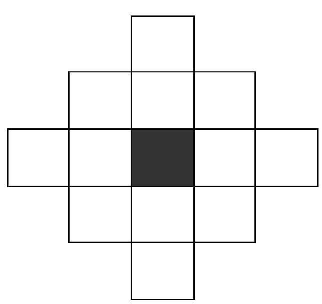

**Figure 4: A diamond-shaped aperture, the black pixel indicates the central pixel.**

All these four complexity measures have similar behavior yet with subtle differences on detailed regions. According to performance evaluation in [8], MAG performs the best for sharpness enhancement and STD is the most effective for coding artifact reduction. In this paper, the implementation of trained filters is based on the classification of ADRC plus STD, which we consider the best for coding artifact reduction.

## 3. Analysis of Trained Filters

### 3.1 Influence of Degradation

Least squares trained filters have been successfully applied on coding artifact reduction [8, 9]. Apart from the classification method, the choice of degradation in the training process also plays a vital role. In this section, we take a close look at the influence of different degradation levels on the performance of the algorithm. We divide the experiment into two parts. In the first part, we use JPEG compression to degrade the original high quality sequences to a wide range of quality levels: from quality 10 to 90 with a step size of 10. The training set contains 25 different sequences, with a large variation of content, including natural-content-based sequences, artificial animated sequences and some film clips, about 2000 frames in total. For each training quality, we get a LUT. Then we apply each LUT separately to a series of test sequences which also have a large variation of quality. Figure 5 depicts snapshots of the three test sequences we use for our experiment. All the test sequences are excluded from the training set. In the second part of the experiment, the main steps remain the same. Instead of JPEG compression, we use MPEG-2 compression for degradation. Default setting is applied for MPEG-2 except that the bit rates are ranged from 0.5M bit/s to 4M bit/s. Apparently, other compression standards, such as H.264/AVC, can be also used for degrading the original sequences. However, those new compression methods already have an in-loop de-blocker to effectively reduce coding artifacts using coding parameters inside the encoder. The purpose of degradation is to simulate sufficient coding artifacts which will be encountered during the filtering process. Therefore, earlier compression standards which produce more artifacts are preferred. Compression artifacts are not the major problem of the latest codecs like H.264/AVC anyway.

**Figure 5: Snapshot of the test sequences: Bicycle, Girlsea and Soccer.**

Figure 6 illustrates performance of trained filters on test sequences with different qualities either compressed by JPEG or MPEG-2, when the LUTs are obtained by varied training qualities.

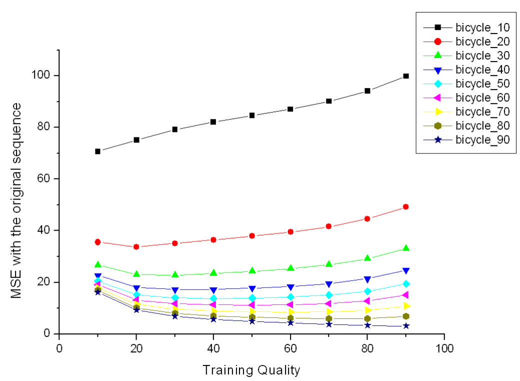


**(a)**

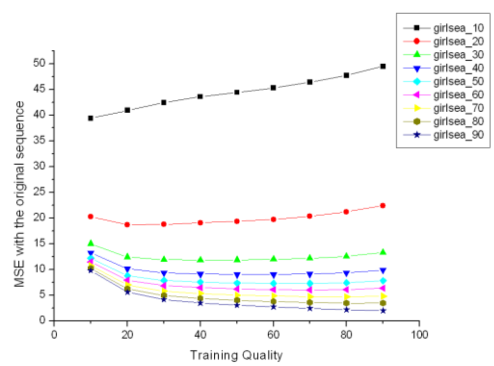


**(b)**

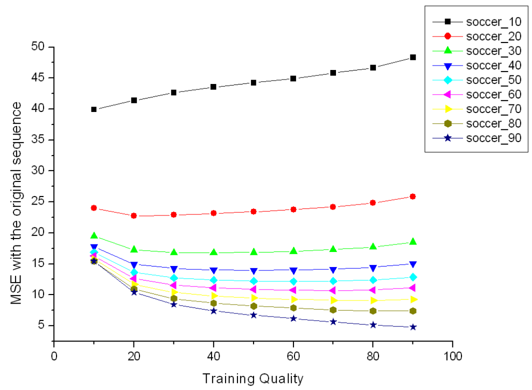


(c)

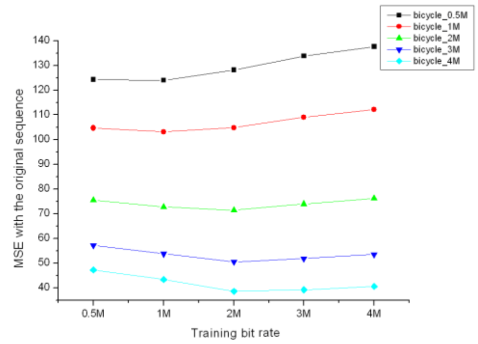


(d)

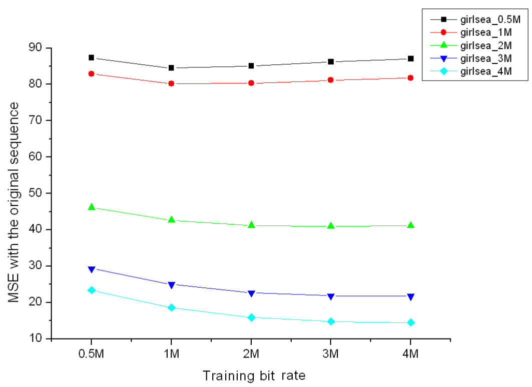


(e)

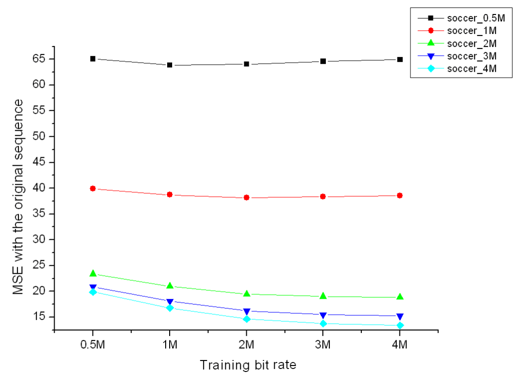


(f)

**Figure 6: Illustration of the influence of different training degradation levels on the output performance. (a)-(c) illustrate different training quality levels vs. MSE scores for the Bicycle, Girlsea and Soccer sequences respectively. (d)- (f) illustrate different training bit rates vs. MSE scores for the Bicycle, Girlsea and Soccer sequences respectively.**

Despite minor differences in MSE behaviors, three test sequences share some common trends. Some observations of the experiment are made as follows:

1. Test sequences with extremely good or bad quality are very sensitive to the choice of degradation during training. For example, for the bicycle sequence compressed with JPEG quality 10, it shows an MSE score of 70.699 when adopting the LUT trained with severe degradation but an MSE score of 99.812 when using the LUT trained with slight degradation. In the latter case, trained filters contribute little improvement to the test sequence. Similarly, for the bicycle sequence compressed with JPEG quality 90, it shows an MSE score of 3.121 when a LUT trained with slight degradation is applied while an MSE score of 16.197 when a LUT trained with severe degradation is utilized.

It is suggested that for high quality input, inappropriate choice of degradation level might blur fine details and thus produce unsatisfying output.

2. Test sequences with moderate quality keep a stable output behavior when LUTs trained with different degradation levels are used. However, we can still easily see from the graphs that the algorithm achieves best performance when the quality of degraded images during training is the closest to that of the test sequence.

However, in most cases, the quality of an input sequence is unknown. So it is difficult to choose the matched LUT beforehand. As a compromise, we use a mixture of uniformly distributed training degradation levels: from quality 10 to quality 90. As expected, it shows better results on the average. In particular, it eliminates the most unmatched cases, which improve the worst case performance. Let us take the Bicycle sequence as an example, the worst MSE score is 99.812 but is improved to 79.513 if we use a mixture of degradation levels in the training process.

### 3.2 Influence of Compression Methods

In this section, we explore the correlation between the type of compression methods used during the training process and the performance of trained filters. Perceptually, we consider that for the Soccer sequence JPEG quality 50 is comparable with MPEG-2 bit rate 1M and JPEG quality 80 is comparable with MPEG-2 bit rate 3M. For MPEG-2, a standard implementation with default setting is adopted. Figure 7 depicts the results on the Soccer sequence. Figure 7(a) shows the result of training on JPEG quality 50 and applying on the Soccer sequence compressed at different qualities by either JPEG or MPEG-2; while Figure 7(b) illustrates the result of training on MPEG-2 bit rate 1M and testing on the same sequence coded by both codecs at different qualities. Figures 7(c) and 7(d) are similar but trained on training sequences compressed at higher qualities.

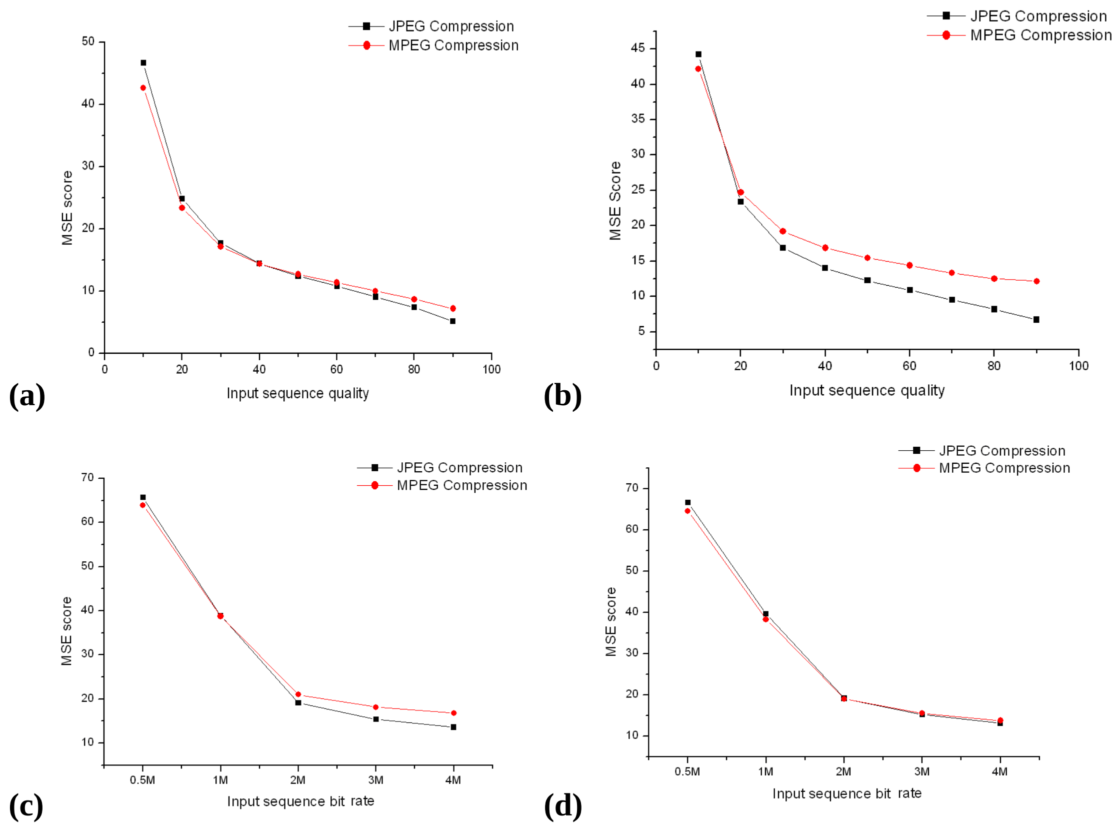


**Figure 7: Illustration of the influence of JPEG or MPEG-2 compression used during the training process. (a)-(b) show the MSE scores, where the training quality for JPEG is 50 and the training bit rate for MPEG-2 is 1M bits/s respectively. (c)-(d) show the MSE scores, where the training quality for JPEG is 80 and the training bit rate for MPEG-2 is 3M bits/s respectively.**

For most cases, JPEG compression shows slightly better performance. The same conclusion can be made on other sequences. These slight differences might arise from the fact that JPEG compression is coded without reference to other pictures in a video sequence. Each frame in JPEG compression is treated independently. So when we set a degradation level for JPEG, the degraded sequence tends to be stable and less variation occurs between frames. However, in the case of MPEG, a hybrid coding scheme that uses both temporal prediction and spatial transformation, i.e., inter- and intra-frame coding, is adopted. Three types of pictures are defined. And only I frames are compressed with intra-frame coding, which behaves in a similar way as the JPEG compression. But the other two types of frames, i.e. B frames and P frames, have a less predictable quality level. For example, the B frames and P frames of two sequences compressed with MPEG-2 using the same bit rate might differ greatly in quality. Furthermore, MPEG-2 standard is flexible with its tolerance about the sequence combination of these three types of frames. Thus in general, the quality of a sequence can be more easily controlled by JPEG than by MPEG-2. As a result, JPEG compression is adopted as the degradation method during training in the following sections.

## 4. Quality Adaptive Trained Filters

From the analysis in the previous section, we understand that the most optimal results can be realized when a LUT whose degradation level during training matches with quality of the input video frame is selected. Careless choice of LUTs might either blur details in high quality images or preserve coding artifacts in low quality images. Thus, a quality control mechanism is required for the trained filters. During training, several LUTs of filter coefficients are produced by using different degradation levels. During filtering, a LUT is selected automatically for each video frame based on its visual quality.

### 4.1 Block Visibility Metric

Since blocking artifact is the most annoying among all the artifacts, a block visibility metric is adopted for measuring the visual quality of an image. This metric is a simplified version of the blockiness metrics proposed in [11, 12]. This approach is highly effective at highlighting block discontinuities and is coherent with subjective perception, while automatically accounting for texture masking effects in a straightforward and computationally efficient manner. Refer to [11, 12] for detailed evaluation of its coherence with subjective perception. The main idea behind the method is that the visibility of block edges does not solely depend on the magnitude of the gradient at the block discontinuity, but it is determined by the magnitude of the block gradient with respect to its neighbors. In other words, block edges are visible whenever the gradient at the edges significantly differs from the gradients in its immediate vicinity. Take the vertical block edges as an example and the horizontal edges can be achieved in a similar way. Consider an image $I$ with element $I_{ij}$, where $i$ and $j$ denote the line and pixel positions, respectively. The absolute horizontal gradient $D_H$ can then be computed by

$$D_H(i,j) = \left| I(i+1,j) - I(i,j) \right| \tag{7}$$

and we simply add up all horizontal gradient for each pixel to S(non-block) and when the pixel position is a multiple of 8 we add it to S(block). Finally, the block grid visibility metric Q is defined as the ratio of the mean accumulated value at the block edge positions and then the mean accumulated value at the non-block edge positions:

$$Q = \frac{S(block)}{S(non-block)} \tag{8}$$

For the three test sequences, we obtain the Q values in Table 1 when they are compressed with different qualities or bit rates.

| **Input File** | **Q** | **Input File** | **Q** | **Input File** | **Q** |
|---|---|---|---|---|---|
| Bicycle_10 | 1.871273 | Girlsea_10 | 2.317374 | Soccer_10 | 3.084992 |
| Bicycle_20 | 1.466661 | Girlsea_20 | 1.706013 | Soccer_20 | 2.213317 |
| Bicycle_30 | 1.334135 | Girlsea_30 | 1.528261 | Soccer_30 | 1.849976 |
| Bicycle_40 | 1.260434 | Girlsea_40 | 1.431847 | Soccer_40 | 1.674414 |
| Bicycle_50 | 1.206434 | Girlsea_50 | 1.358229 | Soccer_50 | 1.556295 |
| Bicycle_60 | 1.161653 | Girlsea_60 | 1.300941 | Soccer_60 | 1.465462 |
| Bicycle_70 | 1.117214 | Girlsea_70 | 1.235921 | Soccer_70 | 1.377247 |

| | | | | | |
|---|---|---|---|---|---|
| Bicycle_80 | 1.074225 | Girlsea_80 | 1.167921 | Soccer_80 | 1.289903 |
| Bicycle_90 | 1.034740 | Girlsea_90 | 1.085089 | Soccer_90 | 1.151064 |
| Bicycle_org | 0.982146 | Girlsea_org | 0.979959 | Soccer_org | 1.000588 |
| **Input File** | **Q** | **Input File** | **Q** | **Input File** | **Q** |
| Bicycle_1M | 2.216744 | Girlsea_1M | 2.710936 | Soccer_1M | 1.597243 |
| Bicycle_2M | 1.838917 | Girlsea_2M | 2.040262 | Soccer_2M | 1.325788 |
| Bicycle_3M | 1.643554 | Girlsea_3M | 1.693213 | Soccer_3M | 1.268037 |
| Bicycle_4M | 1.535949 | Girlsea_4M | 1.511518 | Soccer_4M | 1.234463 |

**Table 1: Measurements of Q value.**

The conspicuous advantages of the block visibility metric are its mathematical simplicity and efficiency and its coherence with visual perception. However, there is a fact that the blocking artifacts are more annoying in flat areas, whereas they are effectively masked in textured area. This fact is illustrated in Figure 8, which shows luminance profiles across block edges for a relatively flat and a textured area. The gradient at block edge is identical in both scenarios. Nevertheless, the discontinuity can be easily identified in Figure 8(a), whereas it is effectively masked by the surrounding activity in Figure 8(b).

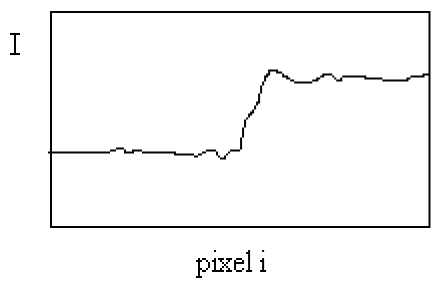


**(a)**

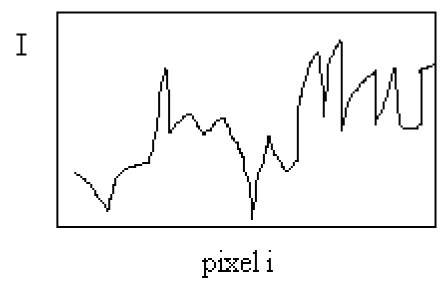


**(b)**

**Figure 8: Luminance profiles across a block edge for flat and textured areas.**

For each sequence, Q values follow strict monotonicity. The larger the Q value, the more severe the degradation of the sequence is. Since it is a blockiness visibility metric, Q value varies across three test sequences, i.e. it is content-dependent. For example, for the same MPEG compression bit rate 1Mbit/s, Q value of the Girlsea sequence arises to 2.710936 but that of the Soccer sequence is only 1.597243. This is in accordance with what we have shown in Figure 8, i.e. the blockiness in the Soccer sequence has been masked by a large area of repetitive grass content, thus gives a relatively low Q value. To make the Q value less content-dependent, we then attempt to set up a threshold for calculation. Take the threshold of 5 as an example. If the luminance gradient of a certain pixel is larger than 5, we just clip it and take 5 as its luminance gradient. We also test other thresholds between 3 and 6, but there are no conspicuous differences. This step is reasonable because some of the luminance gradient arises from the transition in the sequence content, not because of the blockiness. And in most cases, this kind of content transition contributes much more than the real blockiness, which is obviously something we should avoid during calculation. Table 2 shows the Q values with clipping of the gradient. Compared with numbers in Table 1, we can see that the Q values are less content dependent and more stable.

| **Input File** | **Q** | **Input File** | **Q** | **Input File** | **Q** |
|---|---|---|---|---|---|
| Bicycle_1M | 1.683782 | Girlsea_1M | 1.880105 | Soccer_1M | 1.529288 |
| Bicycle_2M | 1.373136 | Girlsea_2M | 1.511507 | Soccer_2M | 1.328376 |
| Bicycle_3M | 1.326298 | Girlsea_3M | 1.413591 | Soccer_3M | 1.293156 |
| Bicycle_4M | 1.299642 | Girlsea_4M | 1.353929 | Soccer_4M | 1.173852 |

**Table 2: Calculated Q values with fixed threshold of 5.**

Based on the above analysis, we decide to use four different levels of JPEG degradation. These include two extreme cases: quality 10 and quality 90 degradation. When Q value of input sequence is larger than 1.83, we use the LUT trained on quality 10 degradation. When Q value is between 1.53 and 1.83, we adopt the LUT trained on quality 20 degradation. When Q value is between 1.25 and 1.53, the LUT trained on quality 50 degradation is applied. The reason we use only one LUT for this relatively large range of quality levels is that they are less sensitive to the training degradation which is concluded from the flat trend in Figure 6. When Q value is smaller than 1.25, the LUT trained on quality 90 degradation is utilized. These thresholds are obtained based on extensive testing and tuning. Machine learning techniques, such as Adaboost [9], can be also programmed to output more optimized threshold values.

## 4.2 Trained Filters Controlled by the Block Visibility Metric

The schematic diagrams of the training and filtering processes of the quality adaptive trained filters are shown in Figure 9.

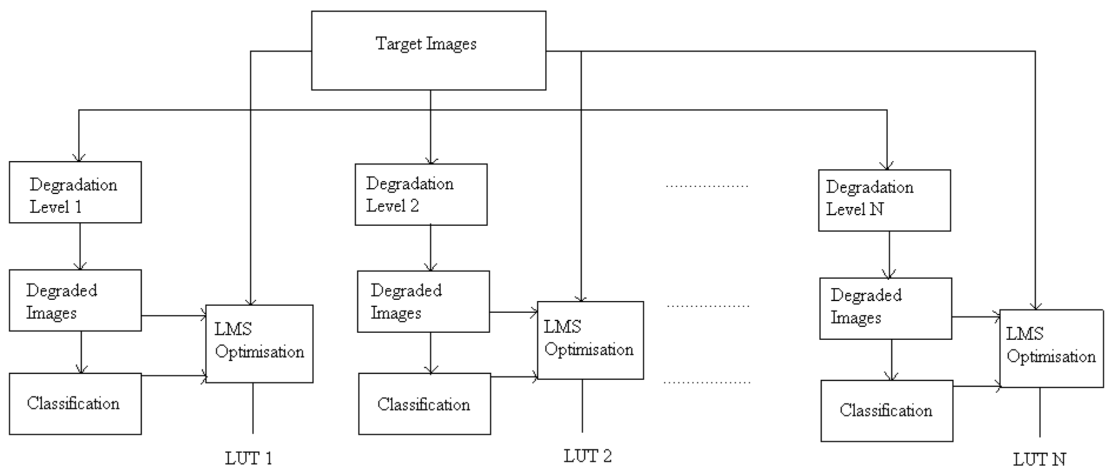


**(a)**

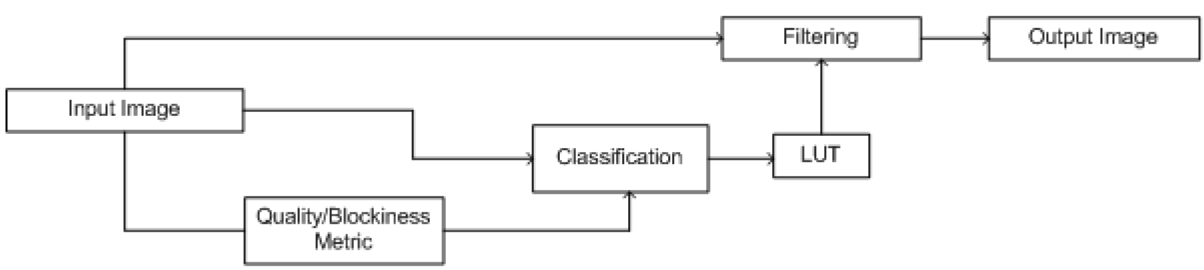


**(b)**

**Figure 9: Block diagrams of proposed quality controlled trained filters. (a) illustrates the training process and (b) illustrates the filtering process.**

We evaluate our quality controlled trained filters with three other post-processing methods [2, 14, 1] for compression artifacts removal. The results of trained filters based on mixed training using degradation levels uniformly distributed from quality 10 to quality 90 are also included for comparison. Three more test sequences as shown in Figure 10 are used for evaluation. All the test sequences are encoded and decoded by MPEG-2 using the default setting. Table 3 shows the resolutions and frame numbers of the test sequences. The MSE scores between original uncompressed sequences and filtered outcomes of the compressed sequences are shown in Table 4. The filtering is only applied on luminance and MSE scores are also only calculated on luminance.

**Figure 10: Snapshot of three more test sequences: Porschefence, Nemo and Vanessa.**

**Table 3: Specification of the test sequences.**

| Sequence | Resolution | Number of frames |
|---|---|---|
| Bicycle | 720x576 | 200 |
| Girlsea | 720x576 | 50 |
| Soccer | 720x576 | 98 |
| Porschefence | 720x576 | 100 |
| Vanessa | 720x572 | 90 |
| Nemo | 720x480 | 512 |

**Table 4: MSE scores of different methods.**

| **Input file** | **Quality controlled trained filters** | **Trained filters - mixed training** | **Ref [2]** | **Ref [14]** | **Ref [1]** |
|---|---|---|---|---|---|
| Bicycle_1M.yuv | 102.726 | 109.812 | 121.850 | 133.539 | 135.750 |

| | | | | | |
|---|---|---|---|---|---|
| Bicycle_2M.yuv | 71.416 | 74.116 | 88.879 | 94.526 | 95.884 |
| Bicycle_3M.yuv | 50.343 | 51.964 | 68.191 | 69.517 | 70.143 |
| Bicycle_4M.yuv | 38.466 | 39.400 | 56.063 | 54.873 | 55.352 |
| Girlsea_1M.yuv | 79.115 | 81.674 | 82.621 | 86.656 | 86.634 |
| Girlsea_2M.yuv | 41.141 | 41.813 | 41.369 | 44.879 | 44.898 |
| Girlsea_3M.yuv | 21.824 | 22.365 | 22.583 | 24.358 | 24.194 |
| Girlsea_4M.yuv | 14.221 | 14.554 | 15.643 | 16.263 | 16.128 |
| Soccer_1M.yuv | 38.862 | 39.359 | 40.243 | 41.297 | 41.137 |
| Soccer_2M.yuv | 18.986 | 19.130 | 20.442 | 20.254 | 20.178 |
| Soccer_3M.yuv | 15.277 | 15.510 | 16.688 | 16.105 | 16.084 |
| Soccer_4M.yuv | 13.105 | 13.634 | 14.709 | 11.439 | 13.892 |
| Porschefence_1M.yuv | 107.429 | 111.974 | 115.505 | 122.428 | 121.984 |
| Porschefence_2M.yuv | 100.013 | 104.175 | 107.487 | 114.490 | 114.152 |
| Porschefence_3M.yuv | 54.396 | 54.516 | 60.735 | 62.758 | 62.673 |
| Porschefence_4M.yuv | 32.019 | 33.428 | 39.866 | 39.411 | 39.036 |
| Vanessa_1M.yuv | 113.048 | 116.749 | 116.314 | 126.095 | 124.230 |
| Vanessa_2M.yuv | 104.498 | 107.611 | 107.187 | 116.804 | 115.115 |
| Vanessa_3M.yuv | 62.880 | 63.473 | 65.402 | 71.741 | 71.202 |
| Vanessa_4M.yuv | 37.833 | 38.272 | 41.052 | 44.891 | 44.323 |
| Nemo_1M.yuv | 97.264 | 98.860 | 101.229 | 104.060 | 103.172 |
| Nemo_2M.yuv | 53.578 | 55.084 | 56.708 | 59.521 | 59.151 |
| Nemo_3M.yuv | 29.312 | 29.734 | 31.812 | 33.346 | 33.110 |
| Nemo_4M.yuv | 18.689 | 19.874 | 22.011 | 22.435 | 22.247 |

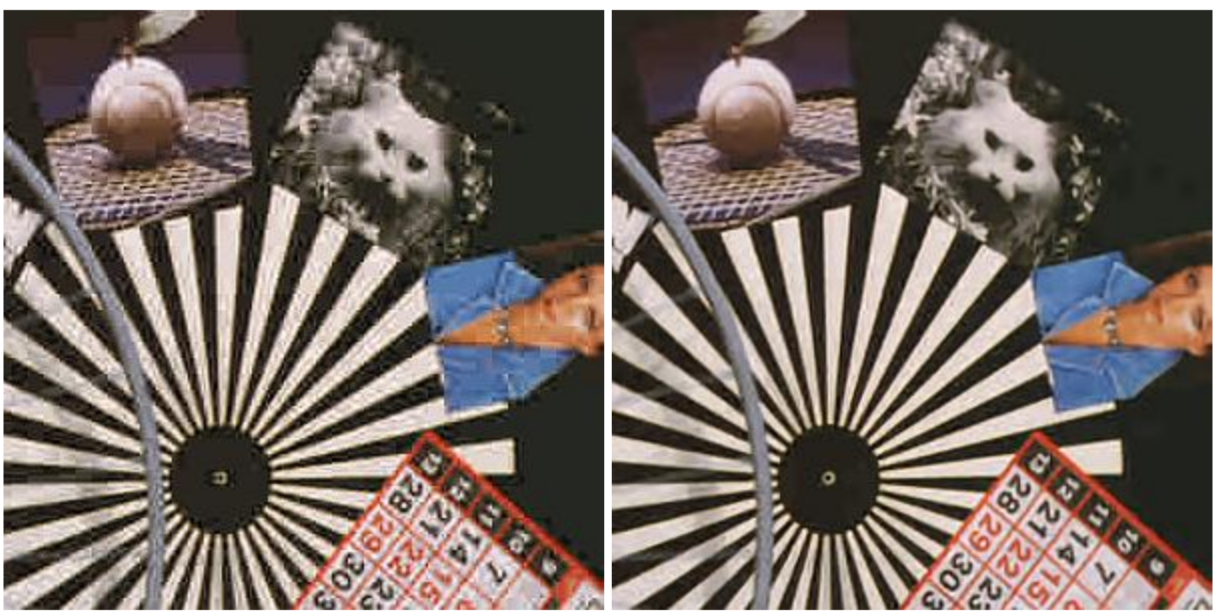

(a) (b)

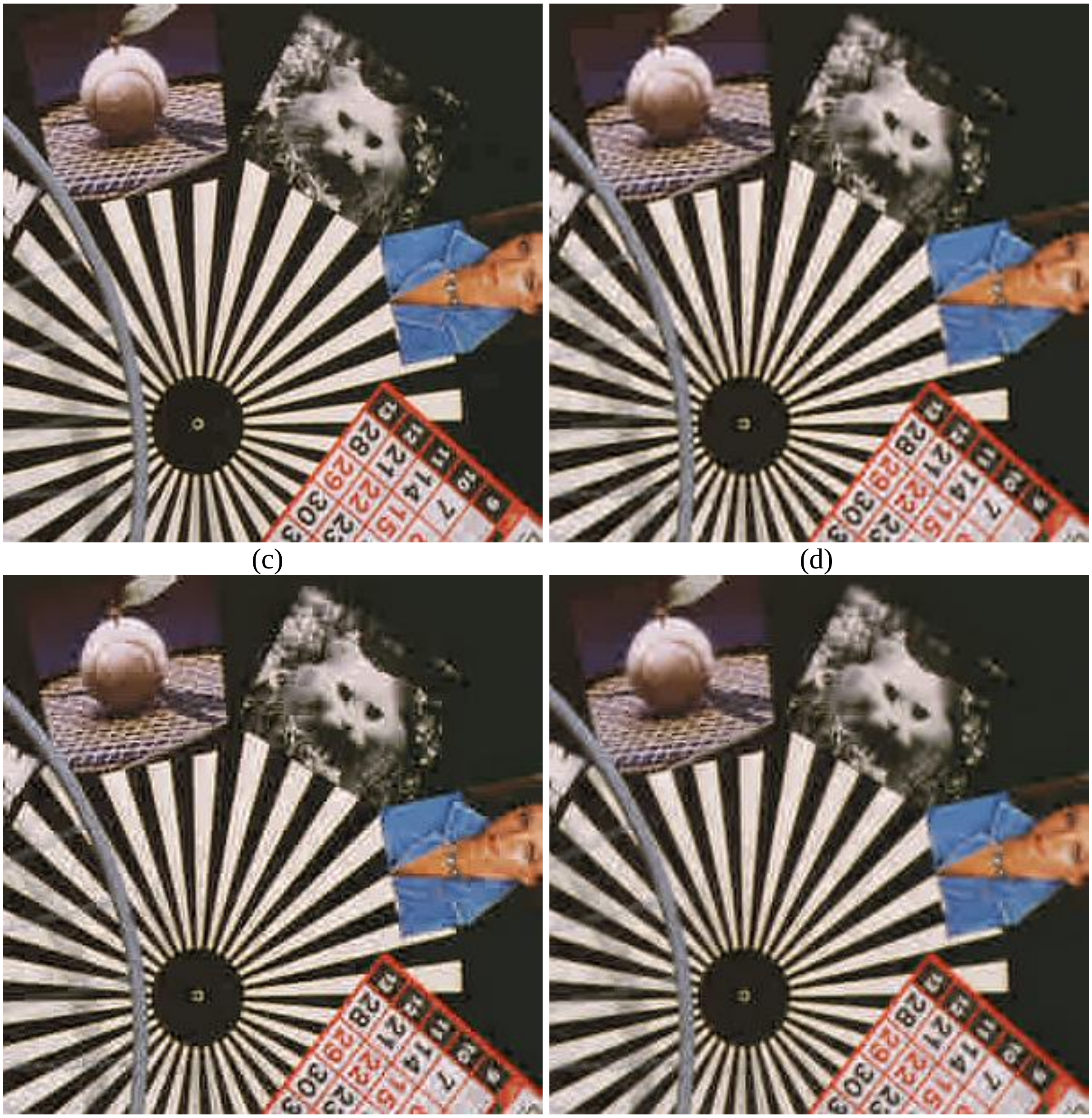

(c) (d)

(e) (f)

**Figure 11: Processed results of the Bicycle sequence: (a) Unprocessed, (b) Quality adaptive trained filters, (c) Trained filters – mixed training, (d) Ref [2], (e) Ref [14], (f) Ref [1].**

We can easily see from Table 3 that the proposed quality controlled trained filters yield satisfying performance. It outperforms the three available de-blocking filters especially in some “difficult” cases, such as the Bicycle sequence and all the sequences compressed at low bit rate.

Besides, compared with the trained filters with mixed degradation, quality controlled trained filters always show some positive improvement.

For subjective evaluation, Figure 11 shows the results of the five algorithms on the Bicycle sequence compressed by MPEG-2 at the bit rate of 1Mbit/s. The proposed quality adaptive trained filters can remove various artifacts and preserve object details better than the other methods. To show some quantitative perception related results, the Structural SIMilarity **(**SSIM) [15] scores of all the test sequences are listed in Table 5. The quality controlled trained filters outperform the three existing methods on all sequences.

**Table 5: SSIM scores of different methods.**

| **Input file** | **Quality controlled trained filters** | **Trained filters - mixed training** | **Ref [2]** | **Ref [14]** | **Ref [1]** |
|---|---|---|---|---|---|
| Bicycle_1M.yuv | 0.3031 | 0.3035 | 0.3039 | 0.2589 | 0.2756 |
| Bicycle_2M.yuv | 0.3334 | 0.3321 | 0.3322 | 0.2785 | 0.2852 |
| Bicycle_3M.yuv | 0.3487 | 0.3467 | 0.3372 | 0.2876 | 0.3134 |
| Bicycle_4M.yuv | 0.3791 | 0.3624 | 0.3536 | 0.2907 | 0.3372 |
| Girlsea_1M.yuv | 0.4261 | 0.4251 | 0.4170 | 0.3589 | 0.3761 |
| Girlsea_2M.yuv | 0.4643 | 0.4562 | 0.4435 | 0.3701 | 0.3953 |
| Girlsea_3M.yuv | 0.4863 | 0.4777 | 0.4636 | 0.3877 | 0.4074 |
| Girlsea_4M.yuv | 0.4998 | 0.4846 | 0.4745 | 0.4035 | 0.4456 |
| Soccer_1M.yuv | 0.3860 | 0.3789 | 0.3698 | 0.3342 | 0.3512 |
| Soccer_2M.yuv | 0.4001 | 0.3991 | 0.3999 | 0.3546 | 0.3662 |
| Soccer_3M.yuv | 0.4153 | 0.4070 | 0.4032 | 0.3754 | 0.3824 |
| Soccer_4M.yuv | 0.4345 | 0.4324 | 0.4279 | 0.3908 | 0.3989 |
| Porschefence_1M.yuv | 0.2851 | 0.2789 | 0.2699 | 0.2345 | 0.2462 |
| Porschefence_2M.yuv | 0.2924 | 0.2894 | 0.2747 | 0.2563 | 0.2641 |
| Porschefence_3M.yuv | 0.3254 | 0.3119 | 0.3012 | 0.2675 | 0.2767 |
| Porschefence_4M.yuv | 0.3459 | 0.3426 | 0.3324 | 0.2990 | 0.2960 |
| Vanessa_1M.yuv | 0.4356 | 0.4292 | 0.4056 | 0.3873 | 0.3936 |
| Vanessa_2M.yuv | 0.4434 | 0.4594 | 0.4361 | 0.4091 | 0.4289 |
| Vanessa_3M.yuv | 0.4776 | 0.4636 | 0.4525 | 0.4094 | 0.4535 |
| Vanessa_4M.yuv | 0.4824 | 0.4724 | 0.4741 | 0.4207 | 0.4671 |
| Nemo_1M.yuv | 0.2730 | 0.2641 | 0.2679 | 0.2463 | 0.2545 |
| Nemo_2M.yuv | 0.2947 | 0.2790 | 0.2741 | 0.2563 | 0.2662 |
| Nemo_3M.yuv | 0.3253 | 0.3220 | 0.3154 | 0.2782 | 0.2873 |
| Nemo_4M.yuv | 0.3425 | 0.3433 | 0.3292 | 0.2943 | 0.3036 |

## 5. Conclusion

In this paper, we develop the classification based least square trained filters for compression artifacts removal using the quality control mechanism. The quality metric we adopt shows robust behavior in blockiness visibility measurement. For an input sequence with unknown quality, the proposed algorithm can choose the most suitable LUT for filtering based on the block visibility metric. The inclusion of the quality control mechanism coupled with the effectiveness of the blockiness metric enables the least squares trained filters to be a decent choice for deblocking images and videos of various qualities.

In future work, a local quality/blockiness metric will be designed to further improve the local adaptability of the algorithm.

## References

[1] L. Shao and I. Kirenko, "Coding artifact reduction based on local entropy analysis", IEEE Trans. Consumer Electronics, Vol. 53(2), pp. 691-696, May 2007.

[2] S. D. Kim, J. Yi, H. M. Kim and J. B. Ra, "A deblocking filter with two separate modes in block-based video coding", IEEE Trans. Circuits and System for Video Technology, Vol. 9, pp.156-160, 1999.

[3] Y. Luo and R. K. Ward, "Removing the blocking artifacts of block-based DCT compressed images", IEEE Trans. Image Processing, Vol. 12(7), pp. 838-842, July 2003.

[4] L. Shao, I. Kirenko, A. Leitao and P. Mydlowski, "Motion-compensated Techniques for Enhancement of Low Quality Compressed Videos", In Proceedings of the 34th IEEE International Conference on Acoustics, Speech, and Signal Processing, Taibei, Taiwan, April 2009.

[5] I. Kirenko, L. Shao, R. Muijs, "Enhancement of Compressed Video Signals Using a Local Blockiness Metric", In Proceedings of the 33rd IEEE International Conference on Acoustics, Speech, and Signal Processing, Las Vegas, USA, March-April 2008.

[6] I. Kirenko and L. Shao, "Adaptive Repair of Compressed Video Signals Using Local Objective Metrics of Blocking Artifacts", In Proceedings of the 14th IEEE International Conference on Image Processing, San Antonio, Texas, USA, September 2007.

[7] T. Kondo, Y. Node, T. Fujiwara and Y. Okumura, "Picture conversion apparatus, picture conversion method, learning apparatus and learning method", US-patent 6,323,905, Nov. 2001.

[8] L. Shao, H. Zhang and G. de Haan, "An overview and performance evaluation of classification based least squares trained filters", IEEE Trans. Image Processing, Vol. 17(10), pp. 1772-1782, October 2008.

[9] L. Shao, H. Hu and G. de Haan, "Coding Artifacts Robust Resolution Up-conversion", In Proceedings of the 14th IEEE International Conference on Image Processing, San Antonio, Texas, USA, September 2007.

[10] T. Kondo and K. Kawaguchi, "Adaptive dynamic range encoding method and apparatus", US-patent 5,444,487, Aug. 1995.

[11] H. R. Wu and M. Yuen, "A Generalized Block-edge Impairment Metric for Video Coding," IEEE Signal Processing Letters, vol. 70, no. 3, pp. 247-278, Nov. 1998.

[12] R. Muijs and I. Kirenko, "A No-Reference Blocking Artifact Measure for Adaptive Video Processing," in Proc. 13th European Signal Processing Conference, Turkey, 2005.

[13] Y. Freund and R. E. Schapire, "A decision-theoretic generalization of on-line learning and an application to boosting", Journal of Computer and System Sciences, Vol. 55(1), pp. 119-139, Aug. 1997.

[14] C. Damkat, “Post-processing techniques for compression artifact removal in block coded video and images”, Technical Report, Department of Electrical Engineering, Technische Universiteit Eindhoven, 2004,

[15] Z. Wang, A. C. Bovik, H. R. Sheikh and E. P. Simoncelli, “Image quality assessment: From error visibility to structural similarity”, IEEE Transactions on Image Processing, Vol. 13(4), pp. 600-612, Apr. 2004.